AERODYNAMIC BASED SHAPE OPTIMIZATION USING CFD: A TRAINING CASE STUDY

Georgios IATROU[1], Anastasios TZOTZIS[2], Panagiotis KYRATSIS[2] and Dimitrios TZETZIS[1]*

*[1]International Hellenic University, School of Science and Technology, 14km Thessaloniki - N. Moudania, 57001, Thermi, Greece, *E-mail: d.tzetzis@ihu.edu.gr*

[2] University of Western Macedonia, Department of Product and Systems Design Engineering, Kila Kozani, 50100, Greece

ABSTRACT: *The present paper deals with the shape optimization of a concept 3-wheeler motorbike geometry designed by Altair University. The geometry was tested in a wind tunnel in the University of Mosbach and the results from this test were used as validating data for a CFD (Computational Fluid Dynamics) simulation that was built and run using the CAE (Computer Aided Engineering) software suite HyperWorks (HyperMesh, Acusolve, Hyperview) provided by Altair. A necessary literature review was conducted for the correct setup of the CFD simulations. The wind tunnel test was simulated and the results showed a satisfactory correlation with the physical test after a mesh independency study. The geometry was then simplified for an external aerodynamics CFD simulation. The settings of the CFD study for the external aerodynamics case, were based on the wind tunnel test simulation setup. The drag coefficient of the 3-wheeler motorbike was estimated and a comparison was made between the resultant drag coefficient of the wind tunnel test and the external aerodynamics simulations. Subsequently, the original model was redesigned. The goal was to improve the original model by reducing the drag coefficient of the vehicle. The new design led to a more streamlined body and on the new geometry, CFD simulations were conducted. These simulations resulted in a significantly lower drag coefficient than the one of the original design. The drag coefficient of the original model was approximately 0.35 and after the redesign process, it dropped to 0.15, a 57% improvement. The reason behind this significant difference is the absence of extensive recirculation areas past the rear of the redesigned model, in contrast with the original design.*

KEYWORDS: *Computer Aided Design, Computational Fluid Dynamics, Computer Aided Engineering*

1 INTRODUCTION

There are many parameters involved in the design of a product. From abstract idea until realization, a product concept goes through several improvement processes until the desirable result is achieved. Some decades ago the only way to test and improve the concepts that lied in the engineers' minds was to construct physical models (that is specifically true for aerodynamics). Nowadays the possibility of designing virtual models of those concepts and test them using computational methods is a standard practice which saves time and reduces the overall engineering costs. One example is the use of Computational Fluid Dynamics (CFD) simulations to study, understand and improve the aerodynamic behavior of a vehicle. CFD is used in automotive, motorsport and aerospace industries among others and its contribution to the design of vehicles has become massive over the last few years. Of course, after a CFD simulation, a physical model is needed to be manufactured and tested in order to validate the results, but still the need of one or two physical models instead of numerous iterations is a great improvement in the research and development sector.

2 LITERATURE SURVEY

Various researchers used wind tunnel experiments and CFD methods in order to study the aerodynamic behavior of ground and air vehicles alike. Such a study was performed by Fintelman et al who employed both delayed detached-eddy simulations (DDES) and Reynolds-Averaged Navier-Stokes (RANS) in order to investigate the flow around a motorbike subjected to crosswinds with yaw angles of 15, 30, 60 and 90 degrees (Fintelman et al, 2015). Authors found that increasing yaw angles result in stronger vortex shedding around the windshield and helmet.

Similarly, Altinisik et al performed experimental and numerical investigations to determine the

pressure distributions and the drag forces on a passenger car model. Experiments were carried out with 1/5th scale model FIAT Linea for 20% and ~ 1% blockage ratios. In addition, three-dimensional, incompressible, and steady governing equations were solved by STAR-CCM+ code with realizable k–ε two-layer turbulence model (Altinisik et al, 2015). Authors stated that the calculated drag coefficients were in good agreement with the experimental results within 6% and pressure coefficients on the model surfaces have shown similar trends in the experimental and numerical studies.

Using similar practices, Skaperdas and Kolovos presented a case study of a CFD model creation for a racing motorbike (Skaperdas & Kolovos, 2007). An investigation on the feasibility of the generation of various mesh configurations and densities with respect to the user effort was made. Only the mesh with the layers was capable of predicting the separation around the rider helmet, showing the importance of the layers presence, when accurate results are required.

Regarding the calculation of the drag effect, Ahmad et al proposed a mesh optimization strategy for accurately estimating the drag of a ground vehicle based on examining the effect of different mesh parameters. The optimized mesh parameters were selected using a Design of Experiments (DoE) method enabling simulations to be carried out in a limited memory environment, and in a timely manner; without compromising the accuracy of results (Ahmad et al, 2010). The study was extended to take into account the effect of model size and based on the authors' findings parameters that lead to drag values closer to the experiment, with less memory and computational time.

Kumar et al presented their work that aims to reduce the drag force which improves fuel utilization and protects environment as well (Kumar et al, 2013). In the stage of work, a sedan car with different types of spoilers were used to reduce the aerodynamic drag force. The analysis was performed for finding out drag and lift forces at different velocities, and implementation of spoilers. Authors proposed an effective numerical model based on the computational fluid dynamics approach to obtain the flow structure around a passenger car with a rear spoiler with the of ANSYS™.

Jain et al studied aerodynamic characteristics of two wheel bikes with the aid of CFD (Jain et al, 2017). According to the authors, in the design stage the designer can evaluate the parameter related to aerodynamics in the basic level of design. At the same time, CFD simulation analysis overcome the previous traditional wind tunnel testing limitation. By the use of CFD numerical simulation the product cycle is short and advantage can be seen in time and cost.

The present paper deals with the redesign of a concept 3-wheeler bike in order to achieve a more aerodynamically efficient shape. To do so, preparation of a CFD model was performed and calculation of the drag coefficient was done. The idea behind this research was to encourage students from mechanical engineering courses to use CFD codes for optimizing their design early enough in the product life cycle.

3 CASE STUDY

At the present study, the main subject is the aerodynamic analysis of the concept model and the improvement of its design. Figure 1 depicts the 3-wheeler motorbike concept, as designed and rendered by the students of Altair University (Altairuniversity.com, 2017).

Fig. 1 Initial 3-wheeler bike

3.1 Modelling methods

Even though the Navier-Stokes equations in their original form can describe a viscous turbulent flow, their use in a solver in the form of RANS (Reynolds averaged Navier-Stokes) is not sufficient to solve the system of equations that are required to describe the flow (Cebeci et al, 2005). The Reynolds stress tensor inserts new unknowns that must be described and calculated. The function of turbulence modeling is to devise approximations for the unknown correlations in terms of flow properties and add the extra needed equations to the system in order to complete it. The "closure problem" as it is described in fluid mechanics literature, has been a subject of investigation for many years. Many turbulence models have been introduced the past few years and they are divided

in algebraic models, one-equation models (for example Spalart-Allmaras) and two-equation models (k-e, k-omega, SST, etc.).
In this project the one-equation Spalart-Allmaras (S-A) turbulence model has been chosen. The Spalart-Allmaras turbulence model is one of the most widely used models in external aerodynamics and turbomachinery. The results that it produces are sufficiently close to experimental results (Tong, 2013). The basic principle is that the Reynolds stresses are correlated with a term called eddy viscosity in order to solve the system of the RANS equations. This term was used by Boussinesq in 1877 to calculate the Reynolds strain tensor in the form of equation 1:

$$\tau_{ij} = 2\mu_T S_{ij} - \frac{2}{3}\rho k \delta_{ij} \quad (1)$$

Where μ_T is the eddy viscosity, $S_{ij} = (\overline{-u_i' v_j'})$ is the turbulent shear tensor, ρ is the fluid density, k is the turbulent kinetic energy and δ_{ij} is the Kroenecker delta.
The Spallart-Allmaras model has a basic form found in equation 2:

$$\rho \frac{\partial(\mu_T)}{\partial_t} + C = F + P - D + T \quad (2)$$

Where C is the convection of μ_T, F is the diffusion of μ_T, P is the rate of production of μ_T, D its rate of dissipation and T its transport by turbulent diffusion. The biggest advantage of the Spalart-Allmaras turbulence model, comparing with the two-equation models, is that it is computationally faster and has proven to be a robust model that provides solid results. It is designed for aerospace applications mainly and gives good results for boundary layers subjected to adverse pressure gradients. However, the S-A model is not calibrated for general industrial flows and produces large errors for some free shear flows. It is also not capable of predicting the decay of homogenous, isotropic turbulence. Unfortunately there is no turbulence model yet that can describe accurately all types of flows and therefore the Spalart-Allmaras model can be accurately used in some cases only.
A low-order panel method has been devised by Mokry for calculating wall interference corrections to the measured drag force in automotive wind tunnels with closed, ¾ open or slotted-wall test sections (Mokry et al, 1995). The method was applied to the Motor Industry Research Association (MIRA) generic car model, tested in three working sections of the German-Dutch Wind Tunnel (DNW), and to three subscale models tested in the DSMA closed-circuit pilot wind tunnel with closed and slotted walls.

3.2 Model development

In the next paragraphs the geometrical models and their preparation for the CFD simulations are analyzed.

3.2.1 Geometry preparation

At this stage, "CAD cleaning" was performed. This term refers to the appropriate preparation of the investigated geometry, before inserting it into a mesh generator.

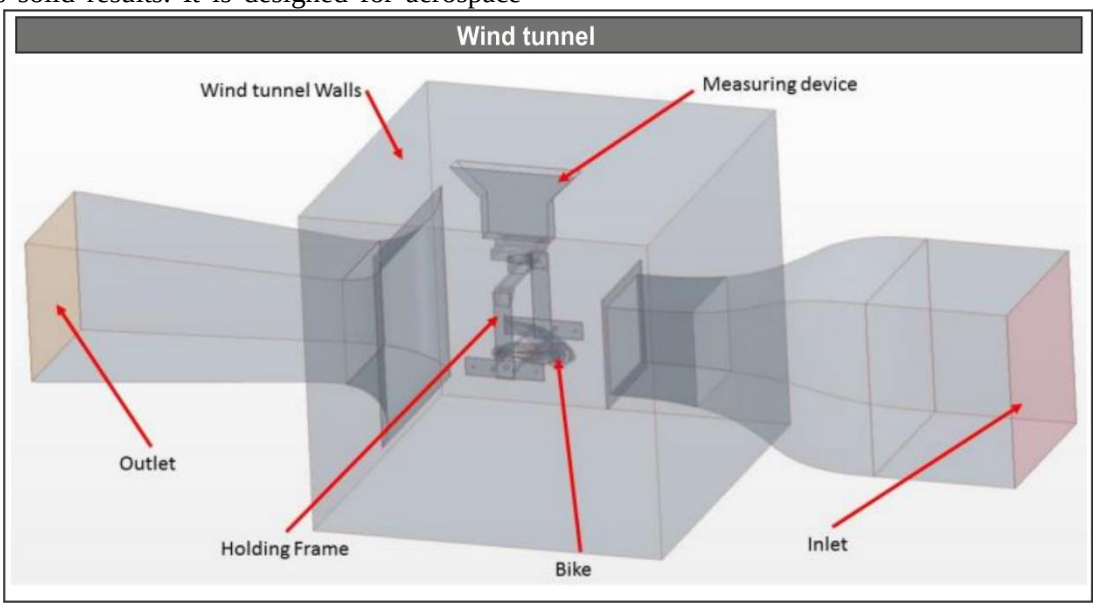

Fig. 2. Virtual model of the wind tunnel

For CFD simulations the most important check regarding the geometry is that it is "water-tight", meaning that the control volume must be closed (sealed) so that the mesh can be generated within geometrical limits. Fortunately, the available tools within commercial codes now allow the use of

several techniques and tricks to facilitate this process. Figure 2 shows the initial CAD file that was provided by the University of Mosbach. This symmetrical model can be split in half in order to save computational time and there is a boundary condition called symmetry that allows that to happen. Therefore, the model was split in half and after some cleaning the final model is shown in Figure 2 (smaller image). The brown surface denotes the symmetry plane. The light blue lines are the points in which the symmetry plane is connected to the rest of the geometry. The process of CAD cleaning was done using the CAD system SolidWorks™.

3.2.2 External flow model preparation

In order to calculate the drag coefficient of the bike, another model needed to be prepared, as the tunnel model includes the frame and other components that disrupt the flow. In the new model, the bike will be examined in an external aerodynamics study. The procedure that was followed to end up with this geometry was to subtract all the wind tunnel parts, the measuring device and the frame and rebuild a domain (control volume) around the bike which will be used for the mesh generation later on. The external flow simulation will differ from a wind tunnel simulation. For example, the boundaries should be far from the investigated geometry CFD code setup. The goal is to achieve a good approximation of the wind tunnel results, using the AcuSolve CFD code. Thus, in the following paragraphs the CFD model setup, the results of the wind tunnel test and the mesh independency study are discussed, in order to choose the correct settings for the next case setup that will investigate the bike drag coefficient (the redesigned model).

3.2.3 Boundary conditions

One of the problems engineers face during simulation setups is that the code cannot always show if the boundary conditions are defined wrong. It is actually rare that the boundary conditions are set so wrong that the code will understand and point it out. If they are not correctly defined, there may be results but will deviate significantly from the reality and the simulation will be useless.

In Figure 3 the boundaries are displayed. The green surface at the right is the inlet. The boundary condition is set in AcuConsole as Inflow with a normal velocity. This means that the fluid (air) flows normally to the inlet with a specific velocity and all the nodes have the same velocity value. The red surface on the other side is defined as Outlet. In the outlet boundary condition, the pressure is set in those nodes to be 0 Pa relative to the ambient pressure. The code will calculate the pressure at the inlet on its own as it will calculate the velocity at the outlet. The light blue surface has a symmetry boundary condition, as mentioned earlier. The symmetry boundary condition acts as a mirror plane. This means that by defining a symmetry, the solver understands that there is the same other half of the domain on the other side of the plane. Using symmetry is a common approach to save a lot of computational time. The rest of the surfaces are defined as walls. The boundary condition "Wall" means that the velocity of the fluid on the nodes that form these boundaries is zero. The solver takes this information in order to form a boundary layer over the walls. The boundary layer existence is critical, since it is the space where the turbulent phenomena start and it is vital for the correct variables' distribution in the field.

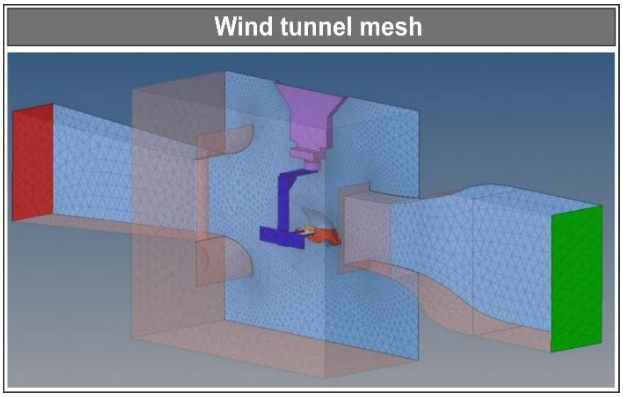

Fig. 3 Wind tunnel domain and boundaries - Surface mesh

3.2.4 Meshing

Before proceeding to the creation of a volume mesh it is important that the surface mesh represents the geometry with an adequate number of elements. Figure 4 (left image) shows the meshed surfaces of the investigated geometry. It is obvious that many triangles are needed in order to have a good representation of this complex geometry. Because of the curvature in many areas, if the mesh is not dense enough then the shape of the meshed surface will be far from desirable and the results will not be representative. On the other hand, an increased number of elements will probably result to large solving times as well. According to Khare et al the accuracy of the simulation strongly depends on the quality of the grid. A good quality grid considering the flow physics leads to faster convergence and better solution (Khare et al, 2009).

Figure 4 (right image) illustrates a section of the initial volume mesh. It is obvious that the mesh is denser close to the investigated geometry and it transitions into a coarser mesh moving further from

the bike, which is a way to improve the mesh locally (in the area of interest). This initial mesh consists of around 384.000 nodes (1.500.000 elements).

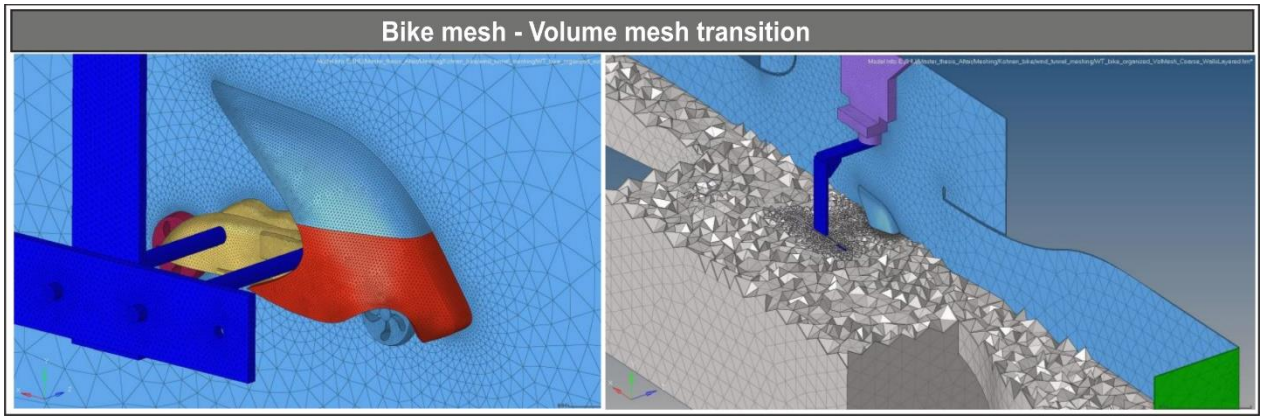

Fig. 4 Bike mesh (left) - Volume mesh transition (right)

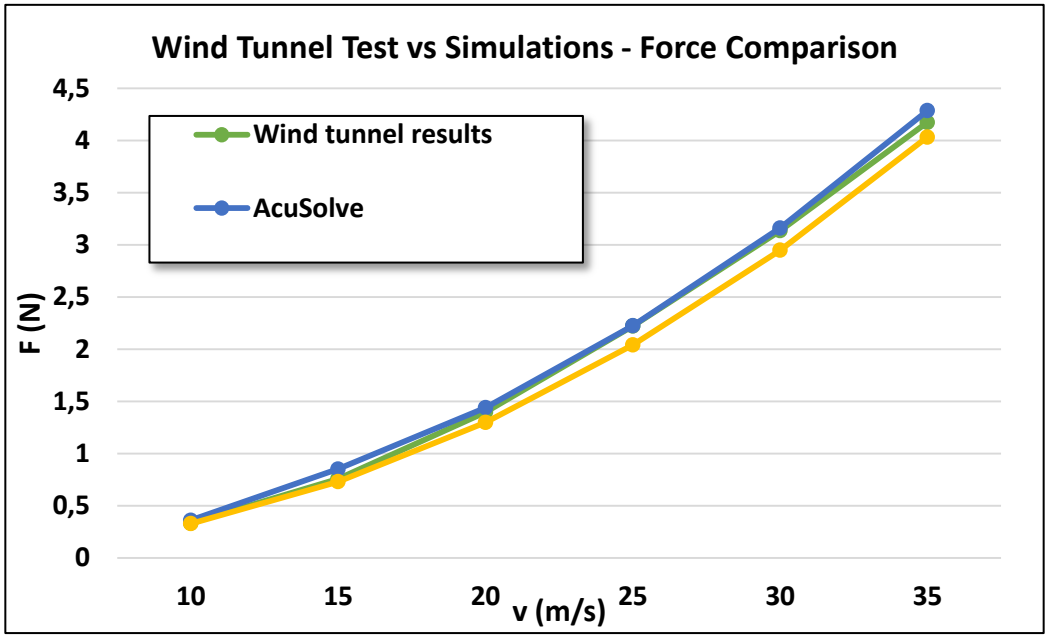

Fig. 5 Wind tunnel test, Wasmeier simulation and Acusolve force estimation comparison

3.2.5 CFD model validation

According to Figure 5, the resultant forces are acceptably close to the experimental results, thus the used settings for the CFD model are acceptable. Specifically, it is understandable that the STAR-CCM+ simulation resulted in less force than the wind tunnel test whereas AcuSolve slightly over predicts the resultant force comparing to the physical test. The resultant force includes the force acting on the surrounding frame.

4 DRAG COEFFICIENT CALCULATION

The bike was subjected to several free stream velocities from 10-40 m/sec with an increment of 5 m/sec. Table 1 contains a summary of the calculated axial force for each simulation. The final row of Table 1 (Total force x2) contains the force that the whole model is subjected to. The "Total force (half model)" row, refers to the forces calculated in the simulation in which half the model was used. The division of the model into its components is shown in Table 1.

According to Table 1, the part that contributes the most in the resultant force, is the bottom part of the fairing as expected. The top part of the fairing comes second with the rest of the parts' contribution being little to negligible. Figure 6 contains the resultant forces of the CFD simulations.

Table 1 Force distribution among bike components (Free stream simulation)

Component	Velocity (m/s)						
	10	15	20	25	30	35	40
	Force in each velocity (N)						
Fairing-top	0.014	0.0315	0.056	0.086	0.125	0.17	0.222
Fairing-bottom	0.0662	0.148	0.2614	0.409	0.585	0.796	1.038
Bike body	0.00092	0.0018	0.002	0.003	0.0025	0.002	0.002
Front wheel	0.0015	0.0033	0.006	0.0085	0.0137	0.0186	0.0243
Rear wheel	0.0008	0.002	0.0044	0.008	0.0127	0.019	0.0285
Total force (half model)	0.08342	0.1866	0.3298	0.5145	0.7389	1.0056	1.3148
Total force x2	0.16684	0.3732	0.6596	1.029	1.4778	2.0112	2.6296

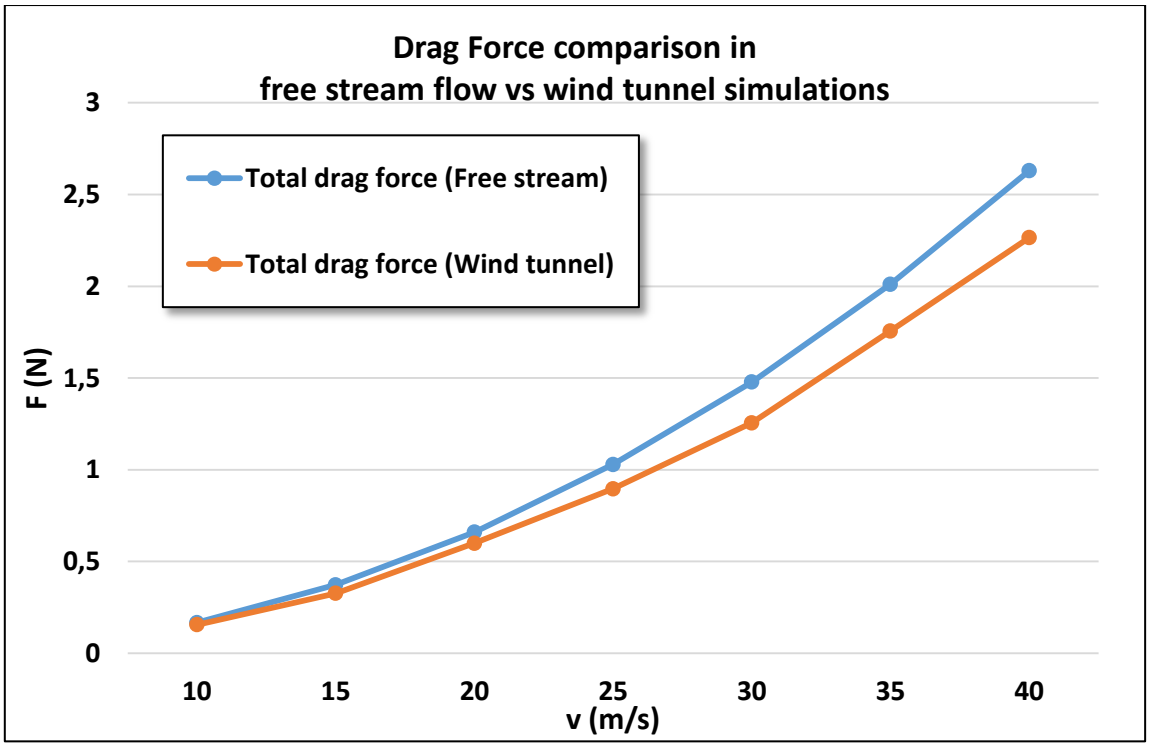

Fig. 6 Comparison between the resultant forces in free stream and wind tunnel CFD simulations

The blue line represents the force that was calculated in the free stream CFD simulation. The orange line refers to the force that acts on the bike in the wind tunnel simulation, which was the one used for validating the CFD code. This force is obtained by subtracting the forces acting on the frame, keeping only the axial force that acts on the bike. This is another advantage of the "organization" of the model's surfaces in several components. The diffusion of the flow as well as the surrounding geometry are obviously effecting the resultant axial force that acts on the bike. The total drag force that is calculated in the wind tunnel simulation is lower than the respective force in a free stream simulation in all velocities.

In order to calculate the drag coefficient C_D there is the need of calculating the forces acting on the geometry D, the frontal area A and the dynamic pressure q_∞ according to equation 3:

$$C_D = \frac{D}{q_\infty A} \quad (3)$$

Measurement SolidWorks™ tool was used for calculating the frontal area value. This value is 3809.49mm^2. In order to calculate this area, a certain procedure was followed; the bike geometry was projected onto a plane. After some corrections in the resultant sketch of the projected area, a planar surface was created and by using the "Evaluate" tool of SolidWorks™, the frontal area was calculated. Since the geometry used in the

simulation is half the model, this area needs to be multiplied by number 2 in order to calculate the frontal area of the complete model.

Table 2 contains the calculated forces of the wind tunnel test CFD simulation, the respective forces of the free stream simulation and the resultant drag coefficients in each case.

Table 2 Drag Coefficient of the original model (simulation results).

Velocity (m/sec)	10	15	20	25	30	35	40
Force (N) Wind Tunnel	0.07	0.1589	0.2811	0.4371	0.627	0.852	1.116
C_D Wind Tunnel	0.3	0.302	0.301	0.299	0.298	0.298	0.299
Force (N) Free Stream	0.08342	0.1866	0.3298	0.5145	0.7389	1.0056	1.3148
C_D Free Stream	0.357	0.355	0.353	0.353	0.352	0.352	0.352

It is obvious from Table 2 that the forces are bigger in the free stream flow case. This difference is translated into the drag coefficient value. In the wind tunnel case, the estimated drag coefficient is around 0.3, whereas in the free stream case this value is approximately 0.35. The difference between the two coefficients was expected due to factors that were explained earlier (flow diffusion in the wind tunnel, surrounding geometry).

5 REDESIGNED MODEL

Figure 7 (upper left image) depicts the redesigned model. The difference from the original model is that the fairing is extended, creating a more streamlined shape. This model approaches the shape of a water droplet; the geometry was designed in SolidWorks™, using automated design techniques (Tzotzis et al, 2017, Kyratsis et al, 2018). This model is expected to result in a smaller drag coefficient than the original model.

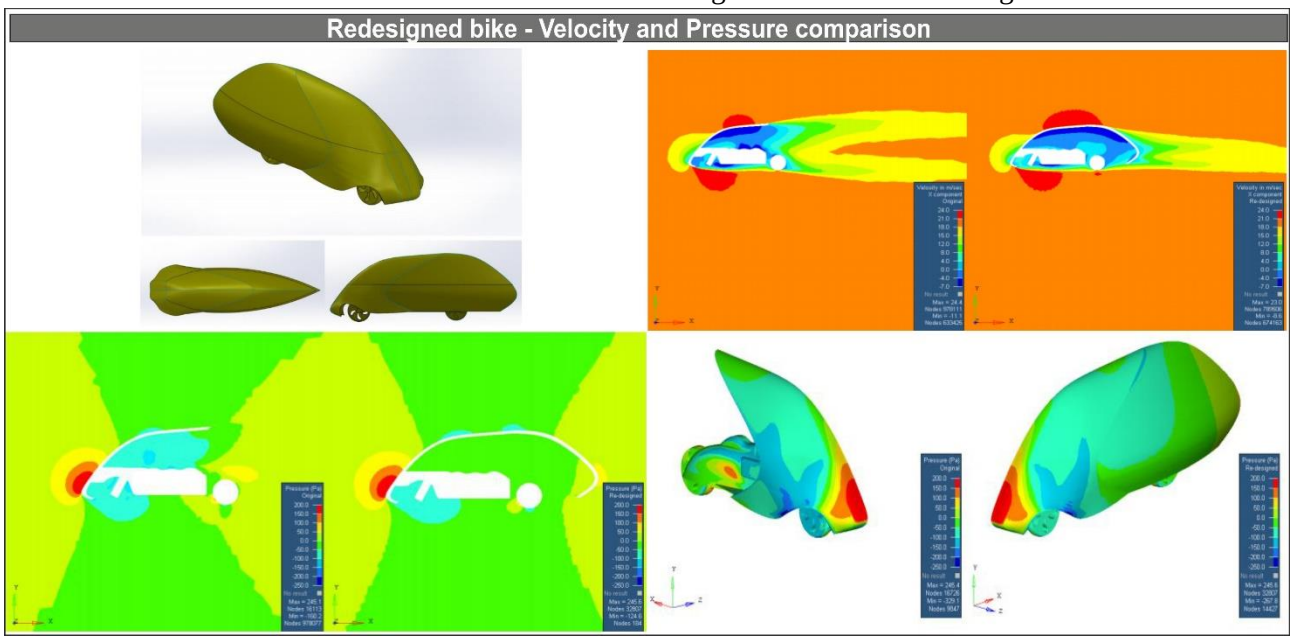

Fig. 7 Views of redesigned model – Velocity and pressure distribution on symmetry plane

The mesh in this case consists of 1,056,404 nodes. The results of this simulation series showed a significant drop of the drag coefficient.

5.1 Pressure and velocity distribution

Figure 7 (upper right image) depicts the distribution of the x component of the velocity around the two models. It is obvious that the redesigned model allows a "smoother" transition of the flow towards the rear of the bike than the original bike. The more disturbed velocity distribution in the original model is a result of the violent detachment of the flow when it reaches the end of the fairing. Big recirculation areas are present therefore in the first case. These

recirculation areas are much smaller in the redesigned case.

Figure 7 (lower left image) shows the static pressure distribution on the symmetry plane. It is noticeable that in the redesigned model case, the pressure is higher under the fairing (one could clarify it more by saying on the "inside" of the bike). This results in less pressure difference between the "inside" and the "outside" of the bike. Therefore the resultant drag force is smaller in the redesigned case, even though the pressure distribution is the same in the front half of the model. Also in Figure 7 (lower right image), the contours do not show much difference on the pressure distribution on the two models' outside surface, however the drag coefficient as we will see is much lower in the redesigned model case.

In Figure 8 (left image), it is shown that several streamlines follow chaotic paths. As a result, the flow behind the model is quite disturbed and vortices are created. Figure 8 (right image) give a good representation of the recirculation due to the new design; the extended fairing of the redesigned model leads the flow towards the rear of the bike smoothly.

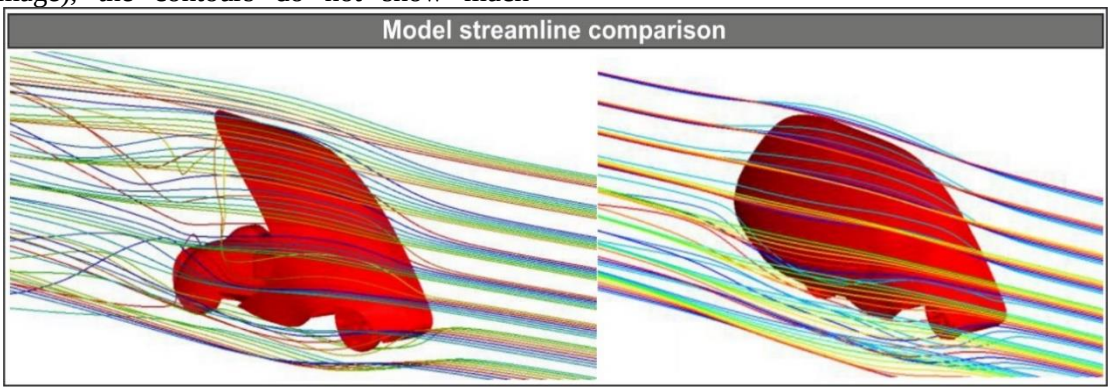

Fig. 8 Model streamline comparison (20 m/sec case)

5.2 Redesigned model drag coefficient

The effect of an aerodynamic design on the drag reduction is being investigated in this section. After running CFD simulations of the redesigned model (for the same free stream velocities as the original model case), the drag forces were measured and translated into the drag coefficient.

Figure 9 contains the results of this study. The drag coefficient has been reduced from 0.35 in the original model, to 0.15 in the redesigned model. The droplet-shaped model is subjected to less than half the drag force of the original model. In the real world this is translated into much less fuel consumption, therefore a much more efficient vehicle.

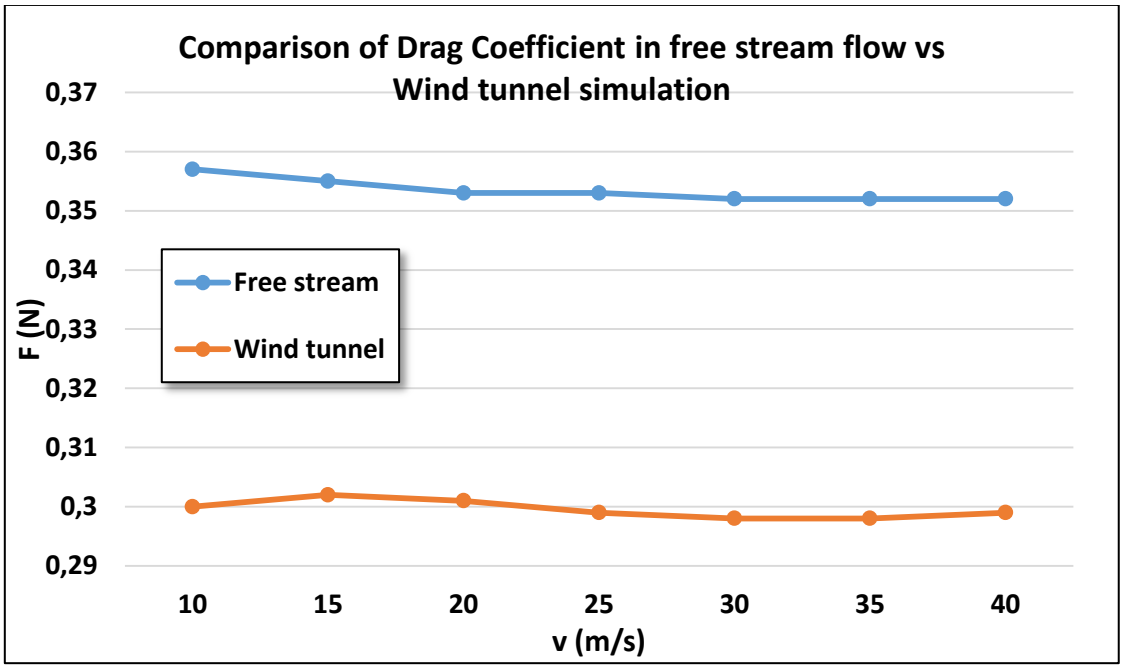

Figure 9 Drag coefficient comparison between the original and the redesigned model.

6 CONCLUDING REMARKS

The process of setting up a CFD simulation is demanding and requires knowledge, experience and attention to detail in order to prove useful for design improvements. No matter how experienced the engineer is, there is always the need of validating the simulation results with measurements in a physical model. In the presented study, the investigated model was the 3-wheeler bike designed by students of the Altair University. Using wind tunnel results from the Baden-Wuerttemberg Cooperative State University of Mosbach, the CFD results were validated through a mesh independency study which led to the correct setup for a computationally cheaper, external flow simulation. The mesh used in the validation process, consists of around 886,000 nodes. The mean value of the deviation between the physical wind tunnel test force calculation and the force calculated in the validation simulation for different velocities, is around 4%, which is an acceptable value.

A free stream simulation was conducted in order to exclude effects from the wind tunnel test structure. The resultant drag coefficient in the free stream, simulation was higher than the one in the wind tunnel simulation. More specifically, the wind tunnel test simulation resulted in a drag coefficient value of 0.3 whereas in the free stream simulation, the value was 0.35. This deviation is justified, since the conditions in a wind tunnel are different than the ones in a free stream (diffusion of the flow after the inlet duct, the supporting frame affects the flow). With the use of CFD, time and physical model building costs are saved, since the simulation results can show which concepts are the most efficient to proceed with. In this case study, the redesigned model, which was based on the 3-wheeler bike, resulted in a significantly lower drag coefficient than the original model. In fact the redesigned model's drag coefficient is 57% lower (from 0.35 to 0.15). The violent detachment of the flow behind the fairing of the original model, leads to a significantly higher drag coefficient than the one of the smoother, droplet-shaped, redesigned model. This outcome can be further investigated using a physical model of the redesigned bike in a wind tunnel test.

7 FUTURE WORK

Many steps of the procedure that is followed to develop and improve a product in terms of its aerodynamic behavior were demonstrated and analyzed in this paper. The results of this procedure can be used as a solid base for the next steps until the realization of a product. The proposed future work consists of some steps that are described as follows. The first step is to conduct a physical test of the redesigned model that will validate the CFD results of this model. Also optimization of the geometry in terms of drag reduction would be very interesting. There are tools that can manipulate the geometry and result to an optimized model, according to constraints defined by the user. The creation and testing of a real-scale model is also anticipated. As vehicle production companies use wind tunnels to test their models, the final stage of the testing is to mount a complete, real model on a wind tunnel and run a test. In that case, the ground should be moving in order to simulate the exact conditions of driving the vehicle. The moving ground can also be implemented in a CFD simulation. These tests will result in a slightly different drag coefficient than the one presented in this case study that will be the real drag coefficient of the 3-wheeler motorbike.

8 REFERENCES

Fintelman, D., Hemida, H., Sterling, M., & Li, F. X. (2015). A numerical investigation of the flow around a motorbike when subjected to crosswinds. *Engineering Applications of Computational Fluid Mechanics*, *9*(1), 528-542.

Altinisik, A., Kutukceken, E., & Umur, H. (2015). Experimental and numerical aerodynamic analysis of a passenger car: Influence of the blockage ratio on drag coefficient. *Journal of Fluids Engineering*, *137*(8), 081104.

Skaperdas, E., & Kolovos, C. (2007). Combining quality, performance & efficiency in CFD preprocessing. In *Proceedings of the 2nd ANSA and META International Congress, Halkidiki, Greece*.

Ahmad, N. E., Abo-Serie, E. F., & Gaylard, A. (2010). Mesh optimization for ground vehicle aerodynamics. *CFD Letters*, *2*(1), 54-65.

Kumar, V. N., Narayan, K. L., Rao, L. N. V. N., & Ram, Y. S. (2013). Investigation of drag and Lift Forces over the Profile of Car with Rear Spoiler using CFD. *International Journal of Science and Research*, *4*(9), 1298-1304.

Jain, I. K. *et al.* (2017) 'Investigation of Drag Coefficient at Low Velocity for Front of Two Wheels Vehicle Based on CFD method', *IJSRSET (International Journal of Scientific Research in Science, Engineering and Technology)*, 3(3), pp. 682–685.

Altairuniversity.com (2017) *Conceptual Design of a 3 Wheeler Motorbike | Altair University*. Available at: https://altairuniversity.com/conceptual-design-of-a-3-wheeler-motorbike/ Accessed: 2018-01-14.

Cebeci, T., Shao, J. P., Kafyeke, F., & Laurendeau, E. (2005). *Computational fluid dynamics for engineers*. Springer Berlin Heidelberg.

Tong, O. (2013). *Verification and validation of the Spalart-Allmaras turbulence model for strand grids.* Utah State University.

Mokry, M. (1995). Wall interference correction to drag measurements in automotive wind tunnels. *Journal of wind engineering and industrial aerodynamics*, *56*(2-3), 107-122.

Khare, A., Singh, A., & Nokam, K. (2009). Best practices in grid generation for CFD applications using HyperMesh. In ATC: HyperWorks Technology Conference 2009 (pp. 1-10).

Tzotzis, A., Garcia-Hernandez, C., Huertas-Talon, J. L., Tzetzis, D., & Kyratsis, P. (2017). Engineering applications using CAD based application programming interface. In MATEC Web of Conferences (Vol. 94, p. 01011). EDP Sciences.

Kyratsis, P., Tzotzis, A., Tzetzis, D., & Sapidis, N. (2018). Pneumatic cylinder design using CAD-based programming. *Academic Journal of Manufacturing Engineering*, 16(2), 107-113.

9 NOTATION

μ_T = eddy viscosity
S_{ij} = turbulent shear tensor
ρ = fluid density
k = turbulent kinetic energy
δ_{ij} = Kroenecker delta
C = convection of μ_T
F = diffusion of μ_T
P = rate of production of μ_T
D = rate of dissipation
T = transport by turbulent diffusion
C_D = drag coefficient
D = drag
q_∞ = dynamic pressure
A = frontal area of model